DOI 10.31489/2023No3/43-51

UDC: 621.43.056; 004.942; 547.218.1

INVESTIGATION OF THE INFLUENCE OF LIQUID FUEL INJECTION RATE ON THE COMBUSTION PROCESS USING KIVA–II SOFTWARE

Berezovskaya I.E., Tasmukhanova A.A.*, Ryspaeva M.Zh., Ospanova Sh.S.

Al-Farabi Kazakh National University, Department of Thermophysics and Technical Physics,
Almaty, Kazakhstan, akhmetovaa2108@mail.ru

In this work, the ignition of liquid fuel was studied at various rates of fuel injection into the combustion chamber. The studied processes are described by the following equations: continuity, momentum, energy, k-ε turbulence model and others. The computational experiment was carried out using the KIVA-II software. The numerical method is efficient and takes into account various factors such as multistage chemical chain reactions, transfer of momentum, heat and mass by convection, radiation, turbulence, etc. In order to select the optimal parameters of the organization of these processes influence of the heptane injection rate into the combustion chamber on the process of combustion and self-ignition of heptane was studied. The injection rate of heptane varied from 160 m/s to 400 m/s an interval of 30 m/s. The size and temperature distributions of heptane droplets before evaporation, the concentration fields of carbon dioxide, and the temperature fields in the combustion chamber depending on the rate of fuel injection through the injector into the combustion chamber were obtained. The optimal range of heptane injection speed was determined, which is 250 m/s - 280 m/s, in order to increase the efficiency of the combustion chamber and reduce the negative impact on the environment.

Keywords: numerical methods, computer simulation, chemical kinetics, liquid fuel combustion, heptane, turbulent heat and mass transfer, injection, combustion chamber

1. Introduction

Combustion processes have been present throughout the history of mankind and surround our daily lives, from heavy industry to the simplest domestic use, passing through all modes of transport, sea, land, air and even spatial. Currently, obtaining energy by burning fuel is essential. Consequently, both in the current geopolitical framework and in the coming years, when fossil fuels become an increasingly scarce resource, its optimal use becomes more and more important every time. But that's not the only thing that matters. Harmful emissions of chemical compounds released during fuel combustion and polluting the environment are the main cause of global environmental problems, especially with the current climate change, as well as the source of many health problems for people living in polluted areas, such as densely populated cities. This means that there is a clear need to optimize fuel combustion processes in order to produce more energy for less, as well as an interest in reducing pollutant emissions resulting from combustion.

These goals can be achieved by studying and improving modern combustion processes present in both domestic and industrial applications such as internal combustion engines or gas turbines. For this, CFD (Computational Fluid Dynamics) modeling can be a very powerful and useful tool. The complexity of numerical modeling lies in the mathematical description of multi-stage processes and physical phenomena such as the evaporation of fuel droplets, the turbulence of the droplet flow.

2. Analysis of the process of turbulent combustion of liquid fuels

Combustion is a complex physical process in which various chemical compounds react exothermically, creating new compounds and heat. The conditions under which combustion occurs (flow rate, turbulence, mixture composition, temperature, etc.) determine the amount of energy and products released during combustion. Let us consider the features of the process of combustion of liquid fuels.

The method of combustion of liquid fuel in the atomized state has the greatest practical application. The process of burning liquid fuels can be divided into the following stages: atomization of fuels using nozzles; evaporation and thermal decomposition of fuel; mixing the resulting products with air; ignition of the

mixture; and combustion itself. Atomization of liquid fuel significantly accelerates its combustion and makes it possible to obtain high thermal stresses in the volumes of combustion chambers by increasing the area of the transition boundary between phases. After entering the heated volume of air, a drop of liquid partially evaporates, while the temperature of the heated air is higher than the self-ignition temperature. Due to the strong radiation of the burning torch, the droplets evaporate very quickly and undergo thermal decomposition. When fuel vapors are mixed with air, a vapor-air mixture is formed. Combustion of liquid fuel occurs in the gas phase. It is the vapors, and not the liquid of liquid fuels, that are flammable, so the liquid only ignites at a certain temperature. Combustion is then maintained spontaneously due to the heat received by the drop from the combustion of the combustible mixture. [1].

Favorable conditions for the rapid heating of fuel droplets are created due to the suspended state in which they are located. Droplet sizes depend on the time of their evaporation and become smaller with time. Also, as a result of assuming a small relative motion due to the viscosity of the gas, the shape of the small droplets becomes close to a sphere. The self-ignition temperature of liquid fuels is always higher than their boiling point, because of this, the combustion of liquid fuels is possible only in the vapor state in the presence of an oxidizing agent [2]. The burning rate depends on the nature of the movement of gases. With turbulent combustion, the mixing of the components occurs more intensively, which significantly increases the combustion rate [3].

3. Basic equations of the mathematical model of the problem of atomization and combustion of liquid fuel

The following are the main equations of the mathematical model of the problem of atomization and combustion of liquid fuel, which includes the equations of continuity, motion, internal energy and k-ε turbulence models.

The unit vectors x, y и z in the directions are denoted as $\vec{\imath}, \vec{\jmath}$ и $\vec{k}$ respectively. The radius vector is defined as $\vec{x} = x\vec{\imath} + y\vec{\jmath} + z\vec{k}$. The vector gradient operator is expressed as follows:

$$\vec{\nabla} = \vec{\imath}\frac{\partial}{\partial x} + \vec{\jmath}\frac{\partial}{\partial y} + \vec{k}\frac{\partial}{\partial z},$$

while the fluid velocity vector has the form: $\vec{u} = u(x,y,z,t)\vec{\imath} + v(x,y,z,t)\vec{\jmath} + w(x,y,z,t)\vec{k}$.

1) The fluid continuity equation is presented in general form, taking into account the chemical term and injection:

$$\frac{\partial \rho_m}{\partial t} + \vec{\nabla}(\rho_m \vec{u}) = \vec{\nabla}\left[\rho D \vec{\nabla}\left(\frac{\rho_m}{\rho}\right)\right] + \dot{\rho_m^c} + \dot{\rho^s}\delta_{m1}, \quad (1)$$

where ρ - the density of the mixture, ρ_m - the partial density of the m-th component, $\vec{u} = (u, v, w)$ - the fluid velocity components, D - the diffusion coefficient, $\dot{\rho_m^c}$- the chemical source term, $\dot{\rho^s}$- source term due to injection, δ_{m1}- Kronecker symbol for the m -th component.

2) The equation of motion for the liquid phase, taking into account droplet evaporation:

$$\frac{\partial(\rho\vec{u})}{\partial t} + \vec{\nabla}(\rho\vec{u}\vec{u}) = -\frac{1}{\alpha^2}\vec{\nabla}p - A_0\vec{\nabla}\left(\frac{2}{3}\rho k\right) + \vec{\nabla}\vec{\sigma} + \overrightarrow{F^s} + \rho\vec{g}, \quad (2)$$

where p – fluid pressure, α – a dimensionless quantity used in the PGS method, which improves efficiency at low Mach number flows where the pressure is uniform; A_0- intermittency coefficient (equal to 0 for laminar flow and 1 for turbulent), k- kinetic energy of turbulence, F^s- speed of impulse return per unit volume due to injection, g – free fall acceleration.

In this case, the viscous stress tensor is found by the formula:

$$\sigma = \mu\left[\vec{\nabla}\vec{u} + \left(\vec{\nabla}\vec{u}\right)^T\right] + \lambda\vec{\nabla}\vec{u}\vec{I}, \quad (3)$$

where μ – the dynamic viscosity of the fluid, λ - the viscosity coefficient, I - the specific internal energy.

3) Internal energy equation:

$$\frac{\partial(\rho\vec{I})}{\partial t} + \vec{\nabla}(\rho\vec{u}\vec{I}) = -p\vec{\nabla}\vec{u} + (1 - A_0)\vec{\sigma}\vec{\nabla}\vec{u} - \vec{\nabla}\vec{J} + A_0\rho\varepsilon + \dot{Q}^s + \dot{Q}^C, \quad (4)$$

where $\vec{J} = -k\nabla T - \rho D\sum_m h_m\nabla\left(\frac{\rho_m}{\rho}\right)$ – the heat flux, T - the liquid temperature, h_m- the enthalpy of the m component, ε- the turbulence energy dissipation, $\dot{Q}^s$- the source term due to interaction taking into account the release of heat per unit of time due to spraying, $\dot{Q}^C$- the source term due to chemical reactions.

4) The standard k-ε turbulence model equation consists of 2 equations:

a) the equation for the kinetic energy of turbulence:

$$\frac{\partial\rho k}{\partial t} + \vec{\nabla}\cdot(\rho\vec{u}k) = -\frac{2}{3}\rho k\vec{\nabla}\cdot\vec{u} + \vec{\sigma}:\vec{\nabla}\vec{u} + \vec{\nabla}\cdot\left[\left(\left(\frac{\mu}{Pr_k}\right)\vec{\nabla}k\right)\right] - \rho\varepsilon + \dot{W}^s; \quad (5)$$

b) equation for the dissipation rate of turbulence energy:

$$\frac{\partial\rho\varepsilon}{\partial t} + \vec{\nabla}\cdot(\rho\vec{u}\varepsilon) = -\left(\frac{2}{3}c_{\varepsilon_1} - c_{\varepsilon_2}\right)\rho\varepsilon\vec{\nabla}\cdot\vec{u} + \vec{\nabla}\cdot\left[\left(\left(\frac{\mu}{Pr_\varepsilon}\right)\vec{\nabla}\varepsilon\right)\right]\frac{\varepsilon}{k}\left[c_{\varepsilon_1}\vec{\sigma}:\overrightarrow{\nabla}\vec{u} - c_{\varepsilon_2}\rho\varepsilon + c_s\dot{W}^s\right], \quad (6)$$

The expression $\left(\frac{2}{3}c_{\varepsilon_1} - c_{\varepsilon_2}\right)\rho\varepsilon\vec{\nabla}\cdot\vec{u}$ takes into account the length of scale changes when there is velocity propagation, and the value $\dot{W}^s$ arises due to interaction with the atomizer. Table 1 shows the standard values of the constants $c_{\varepsilon_1}, c_{\varepsilon_2}, c_s, Pr_\varepsilon, Pr_k$ for the k-ε turbulence model.

Table 1. Values of constants k-ε of the turbulence model.

Constants	Numerical value
c_{ε_1}	1.44
c_{ε_2}	1.92
c_s	1.5
Pr_ε	1.0
Pr_k	1.3

In equations (5) – (6) is:

$$\vec{\sigma}:\overrightarrow{\nabla}\vec{u} = \sigma_{ij}e_{ij}, \text{ where } \sigma_{ij} = 2\mu e - \frac{2}{3}\mu e_{kk}\delta_{ij}. \quad (7)$$

The transfer coefficients can be written as follows:

$$\mu = (1{,}0 - A_0)\rho V_0 + \mu_{air} + A_0\rho c_\mu\frac{k^2}{\varepsilon};\ \mu_{air} = \frac{A_1T^{\frac{3}{2}}}{(T+A_2)};\ \lambda = A_3\mu;\ K = \frac{\mu c_p}{P_r};\ D = \frac{\mu}{pS_c}. \quad (8)$$

Additional terms in equations (1) – (6), which appear due to interfacial exchange and due to chemical reaction, are given in [4].

4. Geometric and physical models of energy fuel combustion

For the computational experiment, a model of a cylindrical combustion chamber with a height h = 15 cm and a base radius r = 2 cm was used. The computational grid consists of 600 cells. The injector was located at the bottom of the chamber in the center, and heptane was injected through it into a preheated oxidizer. The injection occurs unto a stationary medium. The combustion chamber is filled with air. For practical calculations, it is assumed that air consists of 21% oxygen and 79% nitrogen. The injection time of fuel droplets is 1,4 ms. After injection, the fuel rapidly evaporates, and its combustion is carried out in the gas phase. The initial radius of the injected drops is 3 μm. Droplet injection angle is 10º. The pressure in the combustion chamber is $4 \cdot 10^6$ Pa. The area of the injector is $2 \cdot 10^{-4}\text{cm}^2$.

The general view of the model under consideration is shown in Figure 1. The initial temperature inside the combustion chamber was set to 900 K, the temperature of the chamber walls was 353 K. For the study, heptane was taken as a liquid fuel (chemical formulaC_7H_{16}), since it is a mobile and flammable liquid and is used as a reagent and reference fuel in determining the octane numbers of automobile and aviation gasolines.

Mass of injected heptane m = 7 mg. The chemical kinetics of heptane is: $C_7H_{16}+11O_2 \rightarrow 7CO_2 + 8H_2O$. A numerical experiment was carried out using the KIVA-II software with k-ε turbulence model. The injection speed was varied from 160 m/s to 400 m/s with an interval of 30 m/s. Combustion occurs during the transition from the liquid phase to the gas phase and takes approximately 4 ms in time, while the evaporation of fuel droplets takes approximately the first 2 ms [5].

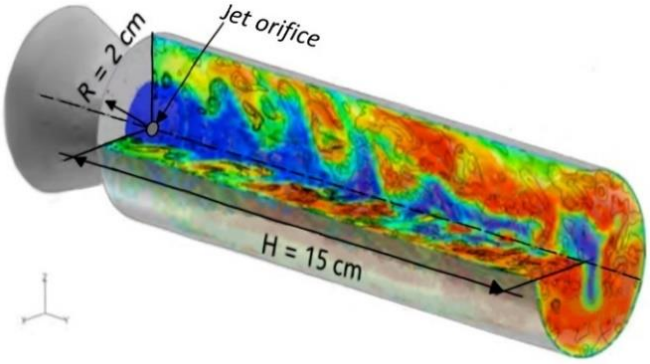

Fig.1. General view of the combustion chamber.

Solving the problem of liquid drops and their interaction with gas phase is an extremely difficult problem. In order to calculate the mass, angular momentum and heat exchange between the evaporating droplet and the gas, it is necessary take into account the distribution of droplets by size, velocity and temperature. In many flows, when calculating sprayed liquids, it is necessary take into account drop vibrations, distortions and discontinuities. For engine calculation, it is also very important to take into account the collisions of drops between themselves and their association into larger drops.

A mathematical model that can explain these complex physical processes, is reduces to the formulation of the evaporation equation. From this the equation is the distribution of the probability density function *f*, having ten independent variables in addiction to time: three *x* positions of the droplet, three components of velocity *v*, radius *r*, temperature T_d (assumed to be the same within the drop), the deviation from the sphere *y* and the change in co deflection time $dy/dt = \dot{y}$. The dimensionless quantity *y* is proportional to the displacement of the surface drop from its equilibrium position to the drop radius *r*.

Physical meaning function f is defined in such a way$f(x, v, r, T_d, y, \dot{y}, t)dvdrdT_d dyd\dot{y}$- probable number of drops per unit volume with coordinate *x* and time *t*, velocities in the interval (*v*, *v* + *dv*), radius in the interval (*r*, *r* + *dr*), temperatures in the interval (T_d, T_d + dT_d) and displacement parameters in the intervals *(y, y + dy)* and ($\dot{y}$, $\dot{y}$ + $d\dot{y}$).

5. Results of a computer experiment of heptane combustion

Below are the results of numerical simulation of the process of burning liquid fuel in the combustion chamber using a stochastic mathematical model, which makes it possible to simulate the effect of the collision of evaporating liquid droplets with aerodynamic discontinuities.

Figure 2 shows plots of fuel droplet size distribution for some injection rates at 2 ms. A qualitative analysis of the graphs revealed that at initial velocities in the range between 160 m/s and 190 m/s, the maximum droplet distribution height of 2.2 cm was recorded, and with a quantitative analysis, at a speed of 250 m/s and above, the droplets spread to a larger volume. Upon reaching 220 m/s and with a subsequent increase in speed to 280 m/s, a sharp drop in height is observed to 1.1 cm, while the number of drops decreases significantly. This is followed by a smooth growth in height up to 1.4 cm. The maximum droplet size was noted at a speed of 220 m/s (fig.2).

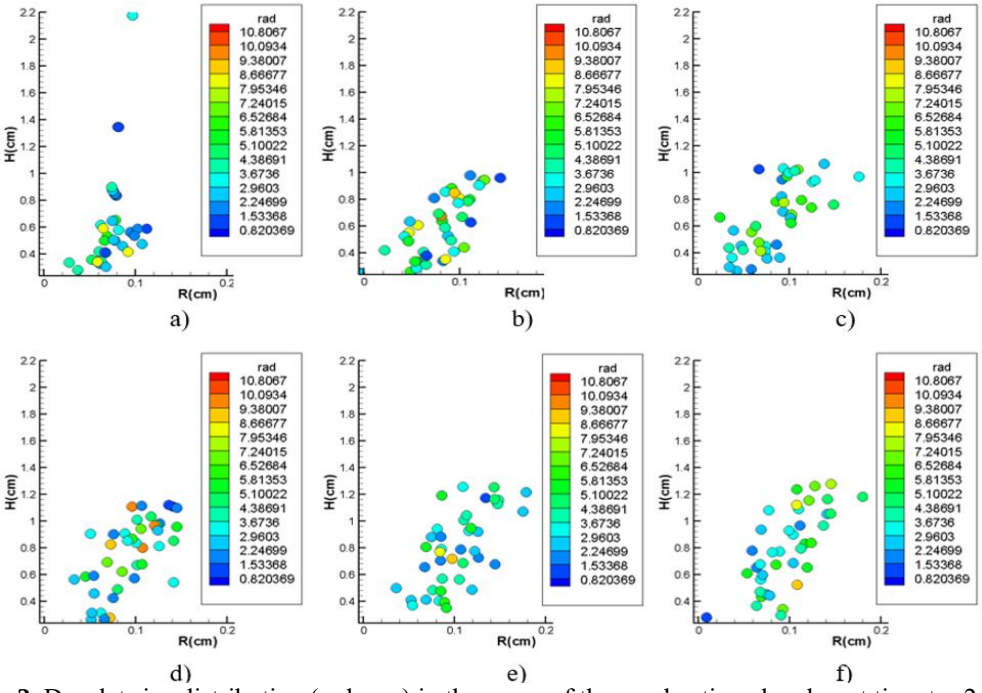

Fig. 2. Droplet size distribution (rad, μm) in the space of the combustion chamber at time t = 2 ms, at injection speed: a) 190 m/s; b) 220 m/s; c) 250 m/s; d) 280 m/s; e) 310 m/s; f) 340 m/s.

Changes in droplet temperature at a time of 0.4 ms with an increase in injection rate are shown in Fig. 3. After 0.4 ms, the temperature of the drops decreases to the boiling point of heptane - 371 K. Quantitative analysis revealed that at the lowest velocities of 160-190 m/s, a huge number of drops are observed with a temperature of approximately 450 K to 485 K. At velocities above 220 m/s droplets have a temperature of 490 K and above. After that, the temperature decreases at 340 m/s to 465 K and below. The highest droplet temperatures were found in the velocity range from 220 m/s to 340 m/s. This means that in this speed range the fuel droplets warm up much faster.

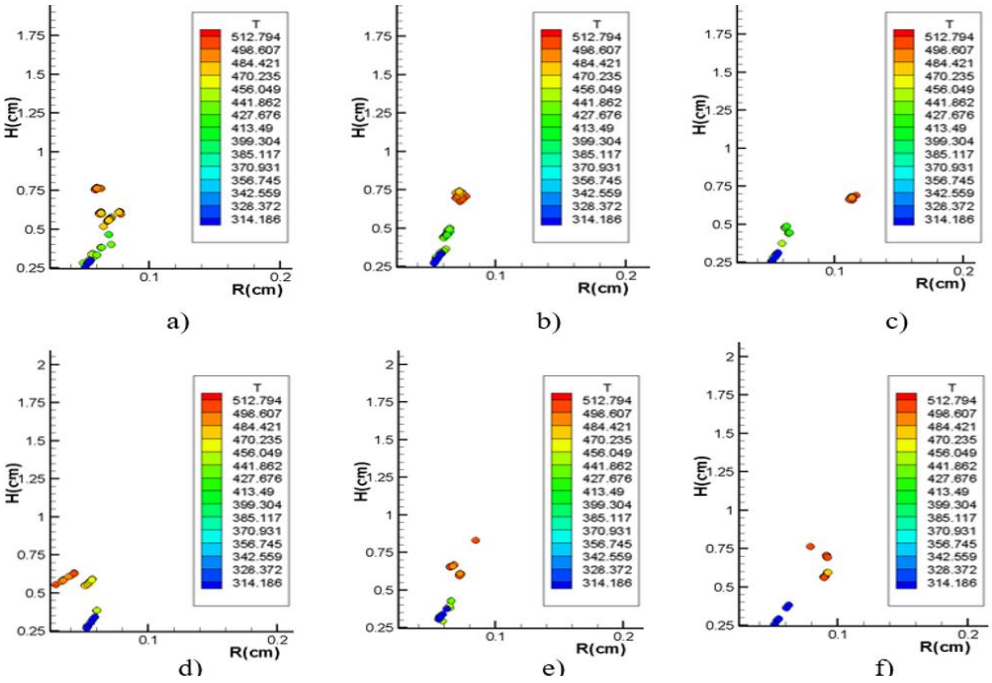

Fig. 3. Graph of droplet temperature change (T, K) at time t = $4 \cdot 10^{-4}$c, at injection speed: a) 190 m/s; b) 220 m/s; c) 250 m/s; d) 280 m/s; e) 310 m/s; f) 340 m/s.

All obtained maximum values of droplet sizes and temperatures at different injection rates are listed in Table 2. Using these data, illustrative line graphs are compiled to track changes in droplet sizes and temperatures at different injection rates of liquid fuel into the combustion chamber, presented in Figure 4.

Table 2. Maximum values of the radius and temperature of heptane droplets at different injection speeds

No.	$V_{injection}$, m/s	R max, μm	T max, K
1.	160	9.57	508.23
2.	190	9.42	506.69
3.	220	10.81	499.11
4.	250	9.98	512.79
5.	280	10.45	505.87
6.	310	9.85	496.26
7.	340	9.91	497.46
8.	370	8.44	464.09

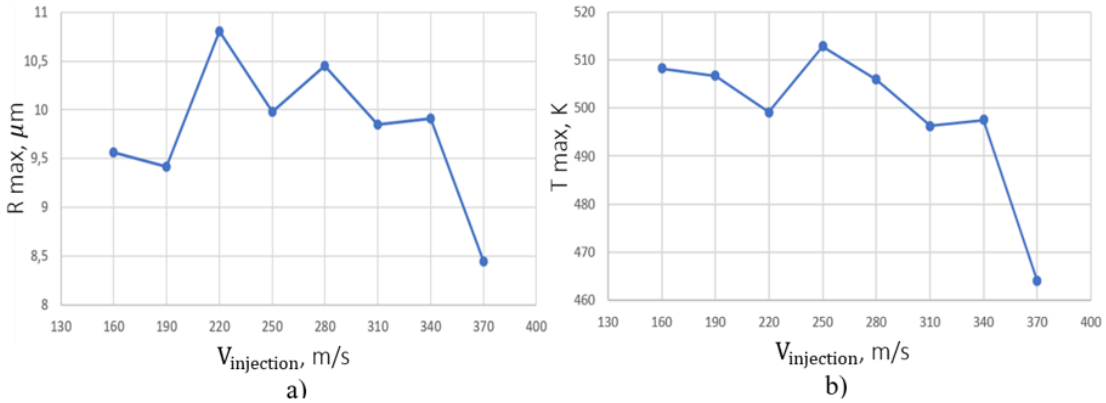

Fig. 4. Line plot of injection speed (V, m/s):
a) on the size distribution of heptane droplets (R, μm) in the space of the combustion chamber;
b) on the temperature distribution of heptane droplets (T, K) in the space of the combustion chamber.

It can be concluded that in the range from 220 m/s to 280 m/s, the droplet sizes increase during mixing, while the number of droplets is much smaller. And, also the distribution of droplets along the height is much lower, in contrast to the data at the initial and final values of the injection speed. The highest droplet temperatures were found in the velocity range from 160 m/s to 280 m/s. This means that in this range of speeds, fuel droplets warm up much faster, respectively, evaporate and ignite faster.

The value stands out strongly on the graph at a speed of 370 m / s, which indicates the need to check these calculations for a miss. The misses were calculated by the Dixon test with a small number of measurements (n<10): $\frac{x_n - x_{n-1}}{x_n - x_1} > Z_q$, where Z_q =0,47, at a significance level q =0.05 for n=8. The known values are listed in Table 3. And below, calculations are made according to the Dixon criterion.

Table 3. Values used for calculations according to the Dixon criterion.

	$V_{injection}$, m/s	T_{max}, K	R_{max}, μm	T'_{max}, K
X_1	355	500.484	10.5786	2187.75
X_{n-1}	365	500.953	9.80386	2194.84
X_n	370	464.091	8.44117	2190.81

a) Checking the value of the maximum temperature of heptane droplets at a speed of 370 m/s:

$$\frac{T_5 - T_4}{T_5 - T_1} = \frac{464.091 - 500.953}{464.091 - 500.484} = \frac{-36.862}{-36.393} = 1.0129 > 0.47.$$

b) Checking the value of the maximum radius of heptane droplets at a speed of 370 m/s:

$$\frac{R_5 - R_4}{R_5 - R_1} = \frac{8.44117 - 9.80386}{8.44117 - 10.5786} = \frac{-1.36269}{-2.13743} = 0.6375 > 0.47$$

c) Checking the value of the maximum radius of heptane droplets at a speed of 370 m/s:

$$\frac{T'_5 - T'_4}{T'_5 - T'_1} = \frac{2190.81 - 2192.94}{2190.81 - 2191.75} = \frac{-2.13}{-0.94} = 2.2659 > 0.47.$$

Since the resulting values are greater than the Z_q value, the results for 370 m/s in this case are a gross error and are not taken into account in the analysis.

The maximum values of the temperature in the chamber and the concentration of combustion product carbon dioxide at various speeds are listed in Table 4. It can be noted that the maximum concentrations of reactants and combustion products released during heptane self-ignition have not practically changed, since the concentration of reactants and combustion products depends on the mass of the injected fuel and the chemical properties of this fuel. In this study, the mass of heptane remained constant for all experiments. The maximum concentrations of nitrogen, oxygen and hydrogen hydroxide at all studied speeds are the same and respectively equal n(N_2) = 0.75 g/g, n(O_2) = 0.1875 g/g, n(H_2O) = 0.06 g/g.

Table 4. Maximum chamber temperatures and concentrations of carbon dioxide for various heptane injection rates.

No.	$V_{injection}$, m/s mm/m/s	T'(max), K	n(CO_2), g/g
1.	160	2166.63	0.1273
2.	190	2163.34	0.1280
3.	220	2167.47	0.1279
4.	250	2181.91	0.1284
5.	280	2181.16	0.1284
6.	310	2180.59	0.1279
7.	340	2188.19	0.1279
8.	370	2190.81	0.1282

The temperature field distributions for each investigated speed are shown in Figure 5 at 4 ms, when the mixture of heptane droplets with air ignites spontaneously.

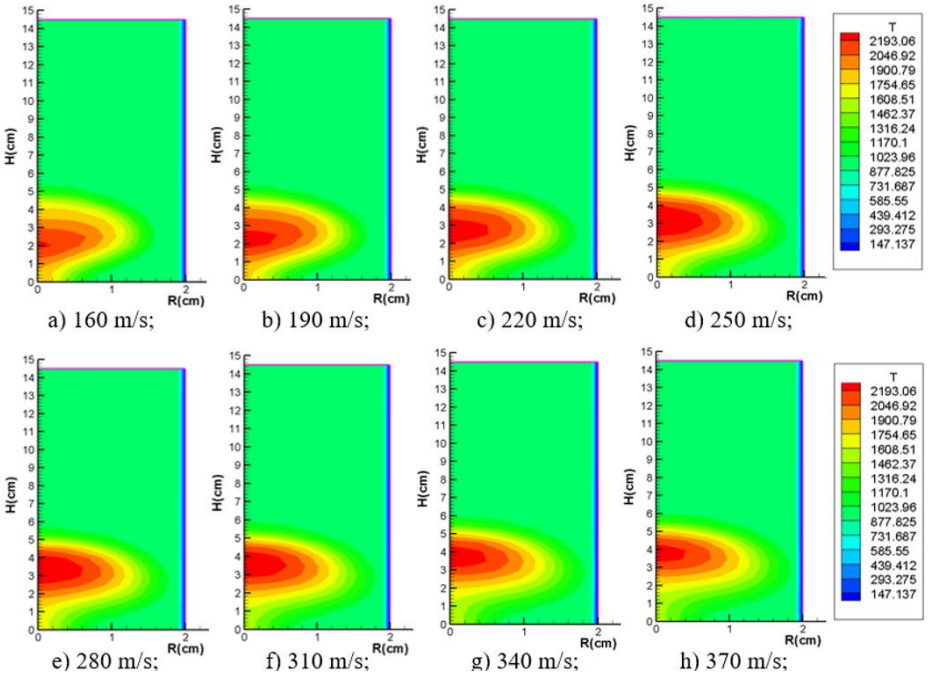

Fig.5. Temperature fields in the space of the combustion chamber at time t = 4 ms, at different speeds.

It can be noted that in the speed range from 250 m/s to 280 m/s, the ignition zone is the largest in area and has the highest temperature. This means that the heptane combustion process is faster and more intense. At lower velocities up to 250 m/s and higher velocities of 280 m/s, self-ignition occurs more slowly and less intensively.

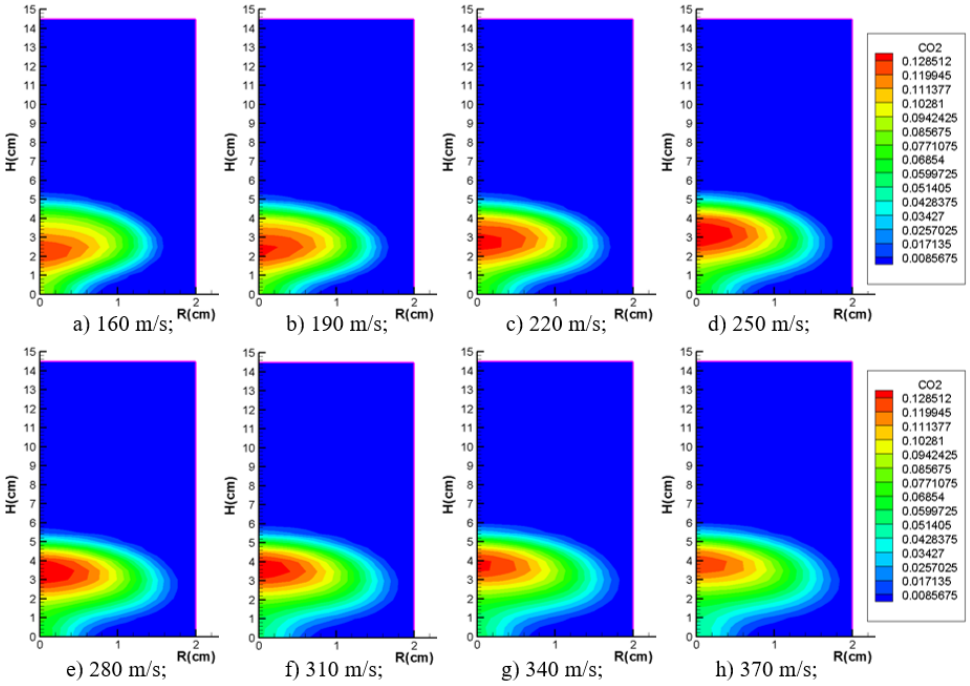

Fig.6. Fields of carbon dioxide (CO_2) concentrations in the space of the combustion chamber at time t = 4 ms, at different speeds.

The figure 6 shows the fields of carbon dioxide concentrations at time t = 4 ms, at different speeds. The largest amount of carbon dioxide was noted at speed in the interval 220 m/s - 280 m/s, but the amount of carbon dioxide released is within the maximum allowable value. This means that at speeds of 220 - 280 m/s, the process of burning liquid fuel proceeds more intensively.

The mathematical model used in numerical modeling in KIVA-II is the basis of the KIVA-3V software. The following authors compared the experiment and numerical modeling, in which the dependence of the torch length on temperature was studied [6]. Figure 7 shows the dependence of the flame length on temperature, on the basis of which it is possible to confirm the agreement between the results of the numerical experiment and the experimental data. Consequently, based on the conclusions of the authors, KIVA-II adequately describes real processes and can be used for research purposes.

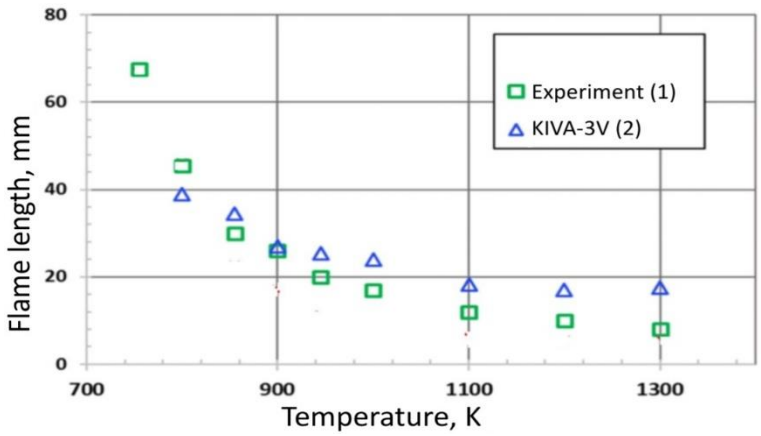

Fig.7. Dependence of the flame length on temperature: 1 - full-scale experiment (Sandia National Laboratories), 2 - numerical experiment (KIVA-3V) [7]

6. Conclusion

In this work, in the course of the study, the distributions of heptane droplets by size and temperature before evaporation, the distributions of the concentration fields of carbon dioxide, and the temperature fields depending on the rate of fuel injection into the combustion chamber were obtained.

As a result of the study, it was revealed that in the range of injection speeds from 250 m/s to 280 m/s, fuel droplets warm up much faster, respectively, evaporate and ignite faster. Consequently, the process of fuel combustion is faster, more intense and more efficient with low fuel consumption.

Research allows choosing conditions for more optimal combustion of heptane, under which the maximum thermal effect of the reaction and small emissions of harmful substances into the environment are observed. The results obtained will not only reduce the negative impact on the environment, but expand the scientific understanding of thermal physics, physics of reactants, thermal power engineering, aircraft and rocket science.

REFERENCES

1. McAllister S., Chen J., Carlos Fernandez-Pello A. *Fundamentals of Combustion Process*. Mechanical Engineering Series, Springer Publication. 2011, 302 p. (Electronic textbook).

2. Askarova A.S., Gorohovsky M.A., Bolegenova S.A., Berezovskaya, I.E. *Numerical modeling of the processes of ignition and combustion of liquid fuels: monograph.* Almaty, Kazakh University. 2015, 124 p. [in Russian]

3. Kowalski M., Żurek J., Jankowski A. Modelling of combustion process of liquid fuels under turbulent conditions. *Journal of KONES Powertrain and Transport*, 2015, Vol. 22, Is. 4, pp.355 – 364. doi:10.5604/12314005.1168562

4. Amsden A.A., O'Rourke P.J., Butler T.D. KIVA-II: A Computer Program for Chemically Reactive Flows with Sprays. *Technical report*. 1989, 180p. doi:10.2172/6228444

5. Askarova A.S., Bolegenova S.A., Voloshina I.E., Ryspaeva M.Zh. Influence of liquid fuel mass on its self-ignition and combustion. *Proceedings of the National Academy of Sciences of the Republic of Kazakhstan. Series of Physics and Mathematics*, 2002, No.2, pp. 3 – 11. [in Russian]

6. *Engine combustion network database*. *Sandia National Laboratories*, USA. 2007. Web. Available at: https://ecn.sandia.gov/engines/

7. Kärrholm F.P., Tao F., Nordin N. Three-dimensional simulation of diesel spray ignition and flame lift-off using KIVA-3V CFD code. SAE *Technical Paper*, 2008, 2008-01-0961. doi:10.4271/2008-01-0961

Article accepted for publication 12.05.2023